

Heat generation and distribution in the ultrasonic hot embossing process

J. Kosloh¹ · J. Sackmann¹ · R. Šakalys² · S. Liao¹ · C. Gerhardy¹ · W. K. Schomburg¹

Received: 22 December 2015 / Accepted: 5 January 2016 / Published online: 22 January 2016
© Springer-Verlag Berlin Heidelberg 2016

Abstract Microstructures are fabricated from polymer foils in seconds by a new process called ultrasonic hot embossing. This process allows to realize new designs within a day and is suitable both for large- and small-scale production. The required investment costs are in the order of some 10,000 €. In this paper, heat generation and distribution in ultrasonic hot embossing is investigated with piezo-electric and pyro-electric foils from the polymer polyvinylidene fluoride (PVDF) placed into a stack of polymer layers. This way, the influence of pre-structures on and powders between polymer layers is revealed.

1 Ultrasonic hot embossing

There are several processes employed for the fabrication of micro structures from thermoplastic polymers such as injection molding, hot embossing, and thermoforming (Heckele and Schomburg 2004). Ultrasonic hot embossing is another molding process developed in recent years (Sackmann et al. 2015). Similar to hot embossing, the polymer to be molded is placed on a tool (cf. Fig. 1a), but the heat required for melting is generated by the sonotrode of an ultrasonic welding machine. The sonotrode presses the polymer onto the tool and heat is generated by ultrasonic vibrations between protruding micro structures on the tool and the polymer, and also between polymer layers if more

than one layer is used (Fig. 1b). The heat melts the polymer and it adapts to the shape of the micro structures on the tool.

Typically either a stack of polymer foils or a polymer plate and a thin foil are employed. It is possible to use only a single plate or foil, but when more than one polymer layer is used, heat is generated also at the interfaces in the inside of the stack reducing the time for melting and molten polymer flows between the layers facilitating taking the shape of the structures on the tool.

Heating of a polymer layer, up to approximately 1 mm in thickness, is achieved in less than a second or at least in a few seconds as a function of the energy required for melting the polymer and an optional auxiliary heating of the tool. After the polymer has been adapted to the tool's shape, the heat is dissipating into sonotrode and tool while the polymer is kept under pressure until it has got solidified again. In the last step of the process, the sample is demolded (Fig. 1c). The separate layers have become a single piece of polymer where they have been molten by the ultrasound. In the area where there are no protruding micro structures on the tool, the ultrasonically hot embossed foils remain as separate layers.

At areas where the polymer has been molten the former layers have undergone a turbulent mixing by the ultrasound. This is demonstrated in Figs. 2a and b. In Fig. 2b the top view of a micro structure fabricated by ultrasonic hot embossing is shown. In Fig. 2a, a cutaway view of a micro structure as shown in Fig. 2b is depicted. At the rim of Fig. 2a the still separated layers from polypropylene (PP) foils in the colors blue, red, and yellow can be identified. At the adjacent area a micro structure has been generated and the mixing of the colors shows the turbulent flow during the process. The Reynold's number of the movement during molding is in the order

✉ J. Kosloh
Kosloh@kemikro.rwth-aachen.de

¹ RWTH Aachen University, KEmikro, Steinbachstraße 53 B, Aachen, Germany

² Department of Mechanical Engineering, Kaunas University of Technology, Studentų St. 56, Kaunas, Lithuania

Fig. 1 Ultrasonic hot embossing

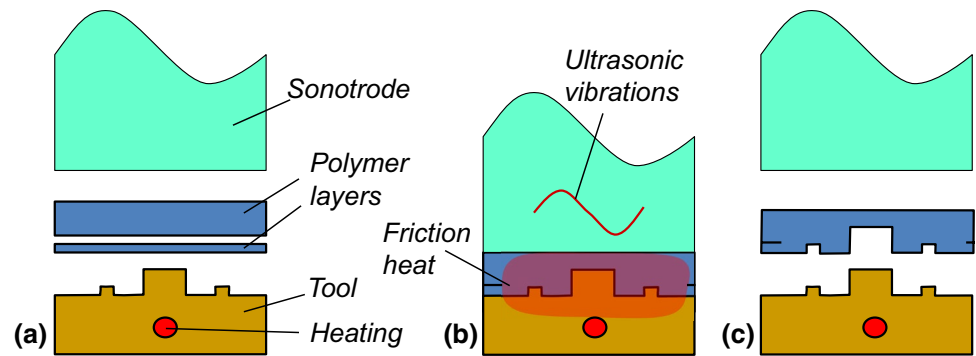


Fig. 2 Top view (b) and a stripe cut out of such a sample (a) of a micro structure ultrasonically hot embossed from a stack of colored PP foils and similar photos after hot embossing without ultrasound (c) and (d)

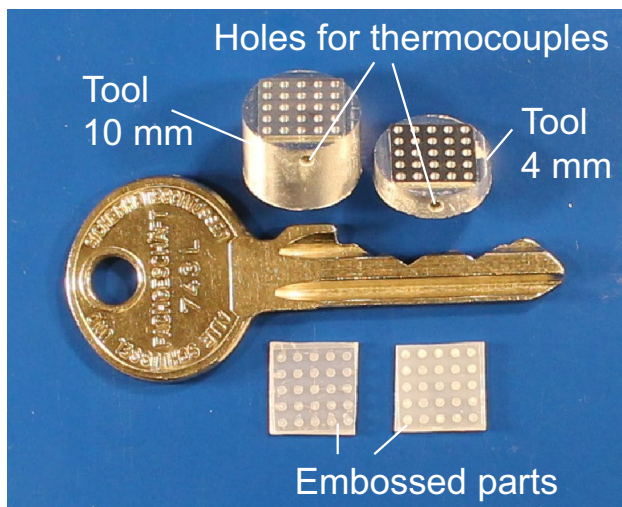
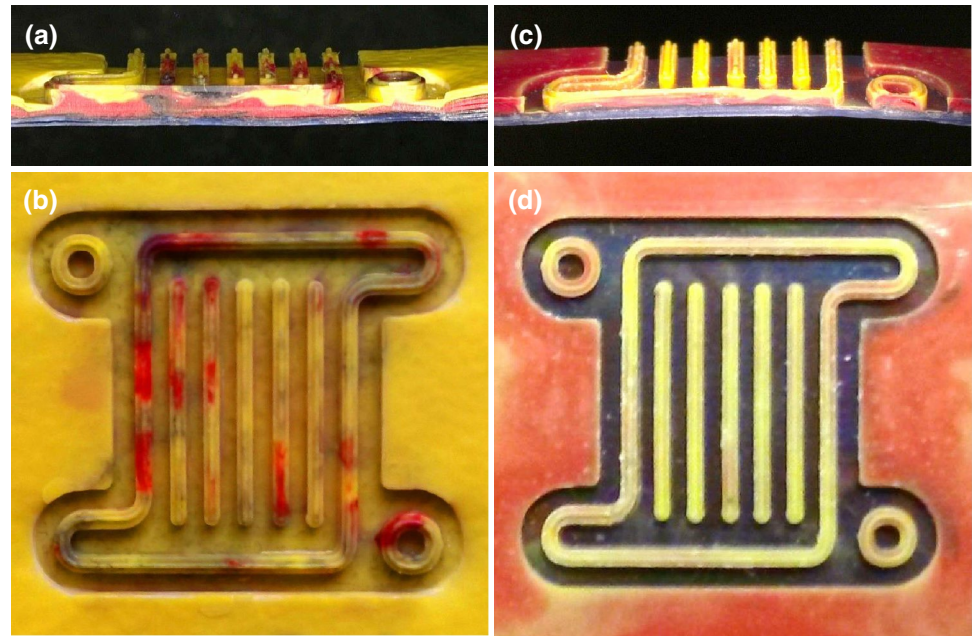


Fig. 3 Aluminum tools, 4 mm and 10 mm in height, and a HDPE sample generated by ultrasonic hot embossing with such a tool

of 10^{-4} and by far too small to explain the turbulent flow. The same kinds of photos were made with a sample from exactly the same polymer layers equally arranged in a foil-stack and with the same tool after hot embossing without ultrasound. This is shown in Fig. 2c, d demonstrating that less mixing of the layers occurs when no ultrasound is involved. For the production of this structure, the mold was heated, and the films were pressed with a press on the tool. In this case, the mold was slowly heated to a temperature of 180 °C. Therefore, the process lasted several minutes, while the preparation of the structure by embossing with ultrasound was carried out within a few seconds.

For all experiments described in this paper, the tools required for ultrasonic hot embossing were milled into aluminum with the milling machine M7 HP from Datron AG, Germany. However, there are several other ways of tool fabrication as described in (Liao et al. 2015).

2 Introduction

Several papers have been published on ultrasonic hot embossing and its variants (Sackmann et al. 2015; Liu and Dung 2005; Mekaru et al. 2007a, b; Khuntontong et al. 2008; Yu et al. 2009; Lee et al. 2010; Altmann et al. 2012; Šakalys et al. 2015; Planellas et al. 2014), but up to now only few investigations have been performed on the physical processes during fabrication. Liu and Dung measured the temperature inside of a polymethylmethacrylate (PMMA) plate, 2 mm in thickness, with thermocouples inserted into drilled holes and discovered that in less than 0.5 s temperatures were rising up to 200 °C (Liu and Dung 2005). Wise measured the temperatures above and aside of an energy director with thermocouples during ultrasonic welding and recorded temperatures as high as 165 °C (Wise 2010). Although ultrasonic molding had its beginning with the molding of plastic powders (Fairbanks 1974; Paul and Crawford 1981), the influence of additive-powders on the process is rarely considered. Planellas et al. found a new method to disperse nanoclays in polymer matrices: They used ultrasonic waves to produce nanocomposites of mixtures of semicrystalline polylactide and polybutylene-succinate plastic powders and nanoclays (Planellas et al. 2014). Since the polymer flow is a strong function of its temperature, the temperature distribution during ultrasonic hot embossing is of large interest. This paper describes investigations of heat generation and distribution during the process. Force and heat distributions were measured by piezo-electric and pyro-electric foils from PVDF between polymer layers and the temperatures in the tools by thermocouples. Moreover the influences of powders between the foil-layers and pre-structures of foils on the ultrasonic hot embossing process are investigated.

3 Temperature generation by ultrasound

When micro structures are generated in a stack of thermo-plastic polymer layers, the ultrasonic vibrations generated by the ultrasonic welding machine are transmitted from the sonotrode into the polymer (cf. Fig. 1b). A part of the ultrasonic energy is transmitted and the rest is reflected at the interface of sonotrode and polymer. The reflected energy is calculated by the reflection coefficient R_{ij} indicating the amplitude of the sound reflected from the interface of material i and j (Sinha and Buckley 2007):

$$R_{ij} = \frac{Z_i - Z_j}{Z_i + Z_j} \tag{1}$$

where Z is the acoustic impedance calculated as the product of sound velocity in and density of the material. As a

consequence of the above equation, the difference of the acoustic impedances of sonotrode and polymer should be as small as possible providing a large transfer of acoustic energy. The reflected energy is proportional to the square of amplitude. The sonotrods of ultrasonic welding machines are typically made of aluminum, titanium, or steel. If high density polyethylene (HDPE) is assumed as the polymer, the corresponding squares of the reflection coefficients R^2 are 0.92, 0.95, and 0.97, respectively. It is obvious that only a few percent of the ultrasonic energy arrives at the polymer.

When the wave front arrives at the tool, it is desirable to reflect as much acoustic energy as possible which then can be absorbed in the polymer. Therefore, a large difference in the acoustic impedance of polymer and tool is desirable.

According to Eq. 1, only little reflection of ultrasound has to be expected at the interfaces between polymer layers. However, when the surfaces of the layers are rough, the enclosed air will reflect ultrasound. Besides this, impedance and absorption of ultrasound by a polymer are a strong function of temperature (Sinha and Buckley 2007), and therefore, increase quickly when the temperature starts rising somewhere.

Also the heat capacity and heat conductivity of sonotrode and tool influence the temperature inside the polymer. In a first step, the temperature in tools was measured with thermocouples inserted into holes drilled 0.5 mm below the micro patterned surface. To improve the heat conductivity between thermocouple and embossing tool, thermal conductive paste (Wakefield) was coated around the inserted end of the thermocouples. As micro structures arrays of holes, 1, 0.35 and 2 mm in diameter, depth, and interval, respectively, were milled into the tops of aluminum cylinders, 14 mm in diameter and 4 and 10 mm in height, respectively. The tools are shown in Fig. 3. Figure 4 displays the temperature measured inside the tools during ultrasonic hot embossing of two foils from HDPE, each 150 μm in thickness. The embossings were performed with the welding machine HiQ DIALOG 1200 from Herrmann

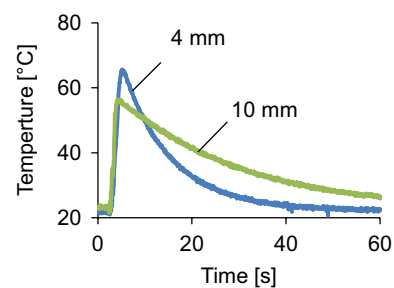


Fig. 4 Temperature measurements obtained during ultrasonic hot embossing employing the tools shown in Fig. 3

Table 1 Parameters of ultrasonic hot embossing processes

Process	1	2	3	4	5	6	7
Ultrasonic welding machine	1	1	1	1	2	1	2
Sonotrode area	□	□	□	□	□	○	□
Amplitude of vibration [μm]	16.3	16.3	16.3	16.3	7.2	30.9	7.2
Force during vibrations [N]	220	650	650	Var.	100	200	100
Duration of vibrations [s]	0.5	0.5	0.2	Var.	0.05	0.5	0.05
Holding time [s]	1	1.5	1.5	1.5	1.5	1	1
Force during holding [N]	150	300	300	300	100	200	100

Welding machines: 1: HiQ DIALOG 1200 from Herrmann Ultrasonics, Germany; 2: Dynamic 745 from Rinco Ultrasonics, Switzerland. Both machines are working at 35 kHz. The sonotrode areas are □: $40 \times 60 \text{ mm}^2$ and ○: circular, 27 mm in diameter

Ultrasonics and the parameters are shown in Table 1 as process 1.

It is expected that the temperature rise is not only due to the heat generated at the interface of polymer and tool but also due to the friction between thermocouple, thermal conductive paste, and tool. However, the different temperatures are expected to be due to the different heat capacities of the tools. The shorter tool becomes warmer because less aluminum is heated up and the faster decrease of temperature is interpreted as a consequence of the shorter way the heat needs to be conducted towards the anvil.

It is concluded from this experiment that the tool for ultrasonic hot embossing should be as thin as possible and have a large thermal conductivity. Besides this, its acoustic impedance should differ much from the one of the polymer. Typically the tools are less than 1 mm in thickness and made of aluminum or nickel but also other materials are possible (Liao et al. 2015). If HDPE is employed as polymer R^2 is 0.92 and 0.97 for tools from aluminum and nickel, respectively.

4 Measurement of the temperature distribution in the polymer stack

The measurement of the temperature inside of a foil stack during ultrasonic processing is hampered because the polymer foils are enclosed between sonotrode and tool, and therefore, cannot be accessed for the measurement of infrared radiation. Besides this, the heat capacity of the polymer layers is comparatively small, and, as a consequence, measurements with thermocouples are subject to a time delay and also biased due to additional friction heat generated at the sensor.

Therefore, the pyroelectric effect (Hesse and Schnell 2014) of polymer foils from PVDF in its β -phase was employed for temperature measurements. Four PVDF foils from Measurement Specialties, 28 μm in thickness, covered with silver electrodes, 5–10 μm in thickness, were

employed. The lateral dimensions of these sensor foils were $12 \times 29 \text{ mm}^2$. The sensor foils were placed between five foils from polypropylene (PP), 200 μm in thickness. Thus, each PVDF foil was enclosed between two PP foils. The polarization of the PVDF foils and the amplification of the output voltage were arranged such, that a pressure applied onto the PVDF foils due to the piezo-electric effect resulted in a positive voltage measured between their electrodes and when the foils were strained in lateral direction, a negative voltage was measured.

Enhancing the temperature of the PVDF resulted in a negative voltage. Measurements showed that temperature shifts of up to 20 $^{\circ}\text{C}$ correspond to a linear relationship to the voltage measured at the PVDF foils of 0.35 V/ $^{\circ}\text{C}$ without amplification.

To prevent destroying the sensor foils, a comparatively small ultrasonic amplitude and force were applied (cf. process 7 in Table 1). The measured voltages are shown in Fig. 5. Sensor foil 1 was placed nearest to the tool and sensor foil 4 nearest to the sonotrode. In the phase I the sonotrode was traveled down onto the foil stack and, as

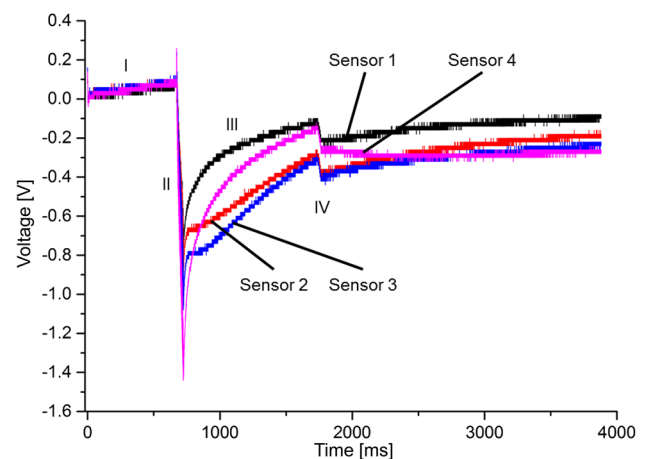
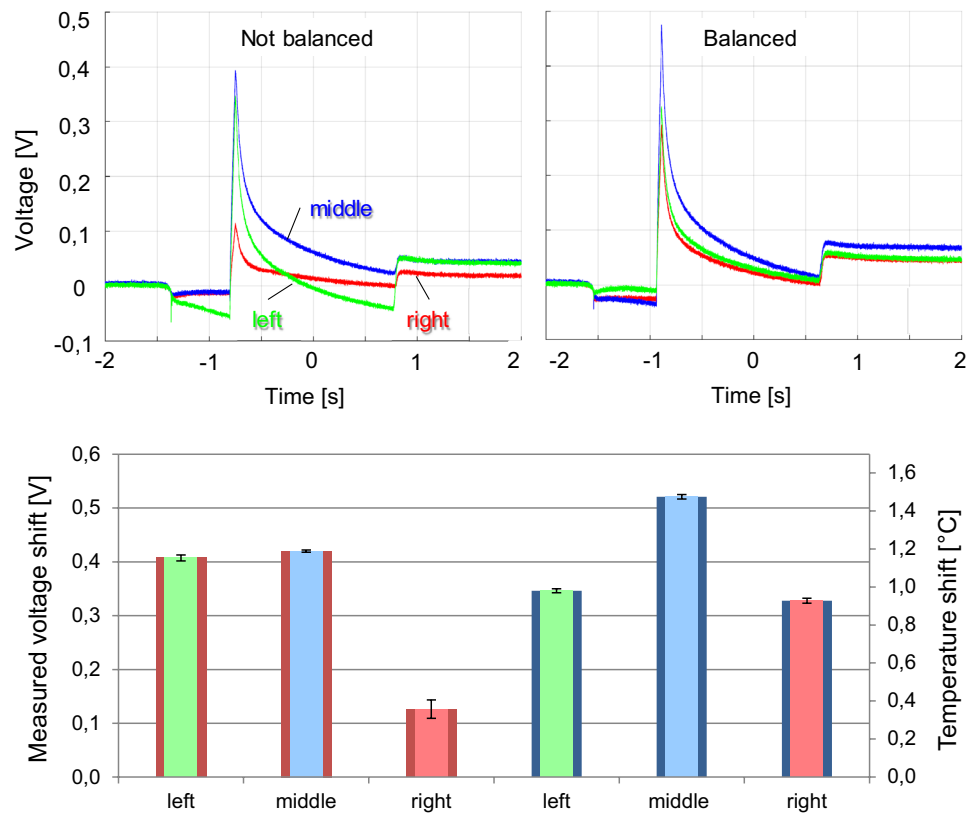


Fig. 5 Voltages measured at four piezo- and pyro-electric PVDF sensor foils placed between five PP foils during ultrasonic processing

Fig. 6 Above: Voltages measured at three piezo- and pyro-electric PVDF sensor foils placed next to each other (*left, middle and right*) between PC-plates during ultrasonic processing. Below: Results of pyro-electric measurements of the same experiment during phase II



a consequence of the piezo-electric effect, the measured voltage was rising. In phase II, ultrasound was applied for 50 ms and the temperature was enhanced by friction heat. Therefore, the measured voltages of all four sensor foils decreased due to the pyro-electric effect. The nearer the sensor foil was to the tool the warmer it got and the more the measured voltage dropped. In phase III, the ultrasound was switched off and the foils were cooling down by heat dissipation. Cooling was fastest for the sensor foils in the near to either the tool or the sonotrode which served as heat sinks. At the beginning of phase IV, the sonotrode was driven up again and the measured voltages dropped due to the piezo-electric effect.

Heat distribution due to applied ultrasound in lateral direction was measured with the next experiment. A PC-plate, 5 mm in thickness, was placed on the anvil, and then followed by three sensor foils from PVDF placed side by side parallel to the shorter edge of the sonotrode. Between sonotrode and sensor foils a PC-plate, 500 μm in thickness, was placed. Ultrasound was coupled into the foil-stack at low parameters (process 5 in Table 1). The results are shown in Fig. 6. The pyroelectric effect is now plotted in positive direction and positive pressure change in negative direction, because the polarity was reversed in this measurement. In the upper part of Fig. 6, two measurement recordings are shown. The measured voltage shifts in phase II and the corresponding temperature shifts are

shown below in Fig. 6. The height of the columns corresponds to the mean value and the error bars are the standard deviation of 3 measurements obtained with the same parameters. The largest error bars correspond to 17 mV as standard deviation.

These measurements show the effect of a non-parallel alignment of anvil and sonotrode. In an unbalanced arrangement (graphs on the left side of Fig. 6), it can be seen that the sonotrode firstly touches down on the left side of the foil-stack. Therefore, the force (100 N total force of the sonotrode) is almost only built up on the left side of the sample, see the negative shift of the left sensor (green) in phase I. Heat is generated almost only on the left side (green) and in the middle (blue) of the foil-stack and much less on the right side, see phase II and measured voltage shifts (left, middle and right) below. Moreover, the pressure relief of the sonotrode at the end of one process is much higher for the left side of the foil stack (see phase IV). In a more balanced arrangement (graphs on the right side of Fig. 6) the sonotrode firstly touches down on the middle of the foil-stack and the pressure is distributed more symmetrically (see phase I and phase IV). Moreover the heat generation is more symmetrically, too, and the maximum voltage shift at all is in the middle of the foil stack, see measured voltage shifts (left, middle and right) below. It is believed that the larger voltage shift in the center of the sample and the corresponding larger temperature rise

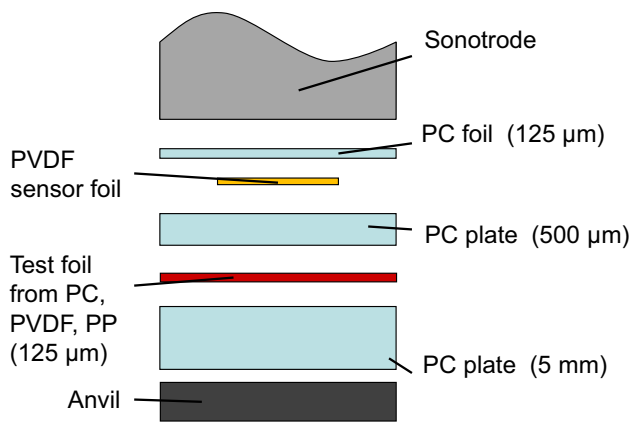


Fig. 7 Design of the foil stack for pyro-electric measurements near the sonotrode as a function of a test foil placed below between PC plates

at this position is due to larger ultrasonic amplitude in the center of the sonotrode. Thus, the measurement of the lateral heat distribution with PVDF foils can be employed to improve the alignment of anvil and sonotrode and to control the homogeneity of ultrasonic vibrations.

Generally, it is noticeable that the voltage shift caused by force relief (beginning of phase IV) is higher than the voltage shift caused by force buildup (phase I). A likely reason for this is that the sonotrode adheres to the material and pulls it in addition to the force relief.

It can be concluded from these experiments that heat generation in lateral direction is maximum under the center of the sonotrode (if anvil and sonotrode are well aligned) and that in normal direction it is maximum next to anvil or tool.

In further experiments, a different arrangement of polymer layers was employed, see Fig. 7. A PC plate, 5 mm in thickness, was placed on a flat anvil without any micro structures. On top of that plate, there were laid a polymer test foil and another 500 μm thick PC plate. Then a sensor foil from PVDF followed and a cover foil, 125 μm in thickness, for electrical isolation to the sonotrode. The 500 μm thick PC plate was placed between test foil and sensor because a distance between them was intended. The measurements were carried out at low forces and ultrasonic power (through setting the parameters as shown for process 5 in Table 1). The voltage drops and corresponding temperature shifts occurring when the ultrasound was switch on in phase II are shown in Fig. 8. The largest voltage change and thus the highest temperature was measured if the test foil was from the same material (PC) as the plates, see the fifth column in Fig. 8.

The temperature change was much smaller if a PP or PVDF foil with the same thickness was employed as the

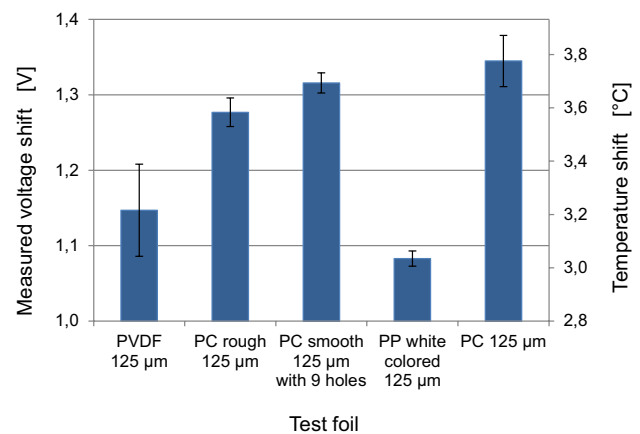


Fig. 8 Results of pyro-electric measurements near the sonotrode during ultrasonic processing as a function of a test foil placed below between PC plates

test foil instead. Employing a rougher PC foil (R_q was about 400 nm on one side and 5 nm at the other side. For the test foil R_q was 3 nm on both sides.) as test foil relates to a smaller but significant temperature change.

Placing a test foil from PC with 9 holes (2 mm in diameter) relates to a non-significant temperature change. It is assumed that air was trapped through these holes of the film. The influence of larger bubbles should be examined in this way.

The smaller temperature rise in the near of the sonotrode measured when a test foil from PVDF or PP was employed may be interpreted such that more ultrasonic power is absorbed at the test foil, and thus less power from the acoustic wave reflected at the anvil can be absorbed at the sensor foil. For semi-crystalline polymers T_g is exceeded at ambient temperature. Thus, the ultrasound is absorbed more (Sinha and Buckley 2007).

The same interpretation may be right for the experiment with a rough test foil resulting in more friction heat generated far from the sonotrode. These results indicate that such modifications of the foil stack help to determine the place and height in the foil stack where the ultrasound is absorbed. Furthermore these results indicate that the ultrasound is transmitted through the stack and reflected at the surface of the anvil. The reflected ultrasound appears to contribute significantly to heat generation. Otherwise a lowering of the temperature in the near of the sonotrode due to more heat generated in a layer 500 μm below the sensor foil is not understood.

Furthermore the same kind of experiment was employed with thicker test plates as test foils from the polymers PC (500 μm), PP (450 μm) and PVC (500 μm). Additionally, measurements were carried out with powder, 50 Vol. % polyethylene wax (PE) and aluminum oxide (Al_2O_3)

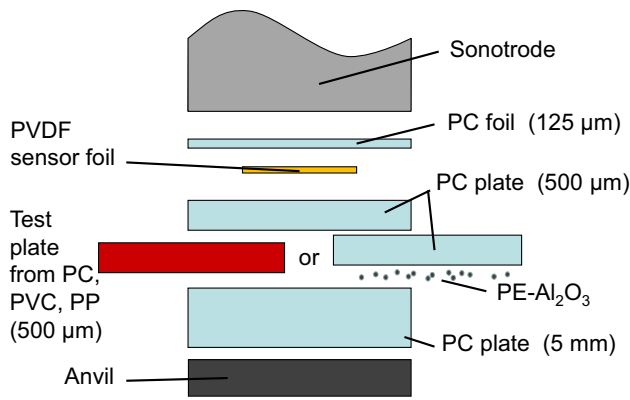


Fig. 9 Design of the foil stack for pyro-electric measurements near the sonotrode while changing test plates and using PE-Al₂O₃ powder in a deeper layer of the polymer stack

(approximately 10–50 μm in diameter), applied under the PC test plate and the result was compared with the same configuration without powder, see Fig. 9.

The observed reduction of temperature rise at the sensor foil becomes larger when a thicker PP plate (450 μm) is used to exchange a PC plate (500 μm), see Fig. 10. The heights and error bars have been derived in the same way as for Fig. 8. In addition, when comparing Figs. 8 and 10, it is remarkable that placing PP or PVDF foils with the thickness 125 μm leads to a stronger reduction of temperature rise than placing an amorphous PC plate which is four times thicker with a thickness of 500 μm.

As test powder PE-Al₂O₃ powder, from the Institute of Mineral Engineering (GHI) at RWTH Aachen was dispersed under the PC test plate, see Fig. 9. In comparison to a otherwise equal configuration, the temperature rise got much smaller when powder was placed under the PC test plate, see Fig. 10. It is believed that the powder has a similar effect as a layer with a rough surface and additionally the short PE chains of the wax may help to generate more heat like a semi-crystalline polymer like PP. Therefore, the powder absorbs more energy from the ultrasound.

These experiments show that the distribution of heat inside of the foil stack can be influenced by placing ultrasound absorbing layers in the foil stack. This way, ultrasonic hot embossing can be facilitated.

All experiments on temperature measurements with pyro-electric PVDF foils were carried out such that no molten polymer was generated.

To prove the influence of powder on ultrasonic hot embossing, micro structures were embossed with smooth PC foils. One foil stack was embossed without powder and one with powder dispersed between all three foils. The same PE-Al₂O₃ powder as used for the experiment shown in Fig. 9 was used. The very dust-like powder had to be carefully dabbed with gloves. By electrostatic attraction it

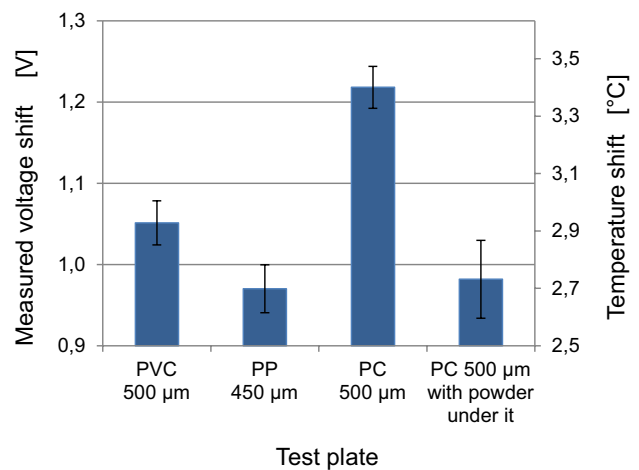


Fig. 10 Results of pyro-electric measurements near the sonotrode while changing just the test plate in the foil-stack and using PE-Al₂O₃ powder

adheres to the PC-foils surfaces. In this way, approximately 1.8 mg of the powder was applied between all foils.

With the chosen parameters (see process 6 in Table 1), it was not possible to emboss the structure if the foil stack was built from three smooth PC foils without any powder in between, see Fig. 11 on the left. The micro grooves on the tool are not completely filled with melt. On the right side of Fig. 11, the same experiment was carried out with powder between the foils and the embossing result is much better although the same parameters were used. The micro channels are completely filled with melt and all energy directors are embossed, too. Thus, the applied powder has a high influence and, in this case, improves the embossing result.

5 Modification of process windows by roughening of polymer foils

Since ultrasonic hot embossing is influenced by the temperature distribution in a stack of polymer layers, the process can be influenced by steering the absorption of ultrasound within the stack. Friction between polymer layers is a function of their roughness because on a rough surface the ultrasonic energy is focused on fewer contact points between the layers. This was investigated by comparing the process windows of even and roughened foils from PC.

Polymer foils with a defined roughness were fabricated by ultrasonic hot embossing of a stack of two PC foils, each 250 μm in thickness, on a tool with micro pyramids, 300 μm in height, with a square base, 450 μm in length. This process was carried out with the ultrasonic welding machine HiQ DIALOG 1200 from Herrmann Ultrasonics.

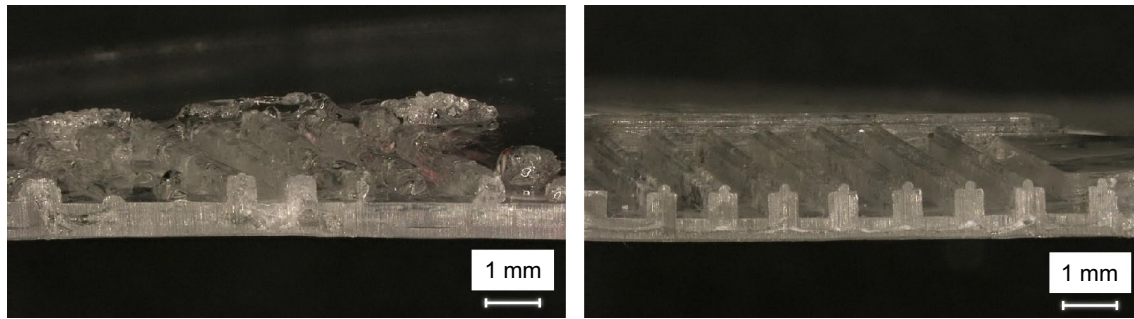


Fig. 11 Cuts through micro structures, ultrasonically hot embossed with the same parameters using a stack of 3 smooth foils, each 250 μm in thickness, without (*left*) and with $\text{PE-Al}_2\text{O}_3$ powder between the foils (*right*)

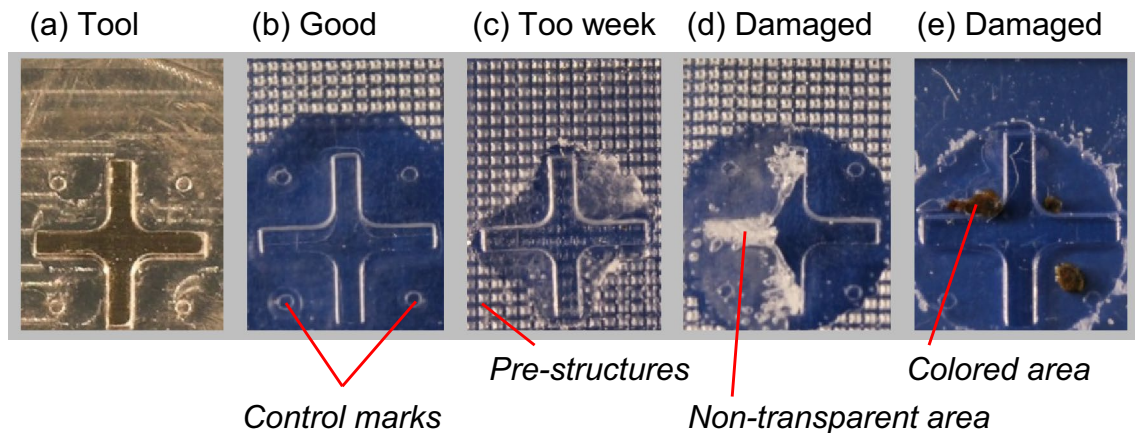


Fig. 12 Aluminum tool (a) and a good (b), too weak (c) and damaged (d) embossing with pre-structured PC foils, and a damaged embossing into PVC without pre structures (e)

The process parameters are shown in Table 1 as process 2. These roughened foils are called pre-structured foils in this paper. Also, pre-structured foils from polyvinylchloride (PVC) were fabricated by ultrasonic hot embossing two foils, 225 μm in thickness, employing the same tool with the parameters shown in Table 1 as process 3.

The pre-structured PC foil, approximately 500 μm in thickness, was then combined together with an even foil, again 250 μm in thickness, in several arrangements for ultrasonic hot embossing. For the tool, a protruding cross bar, 8 mm, 500 μm and 1 mm in length, height and width, respectively, and control marks, 500 and 50 μm in diameter and height, respectively, were milled into aluminum (Fig. 12a). The micro structures generated in a stack of PC or PVC foils by ultrasonic hot embossing with this tool are shown in Fig. 12. An embossed structure was considered as too weak when the control marks were not completely seen (Fig. 12c), damaged when a decomposition of the polymer was recognized either by nontransparent parts (Fig. 12d) or brown or black coloring (Fig. 12e), and good when the

control marks were clearly seen in the polymer and no non-transparent or colored areas appeared (Fig. 12b).

For all experiments described in this chapter, the tool was heated up to 30 $^{\circ}\text{C}$ ensuring that all foils were embossed at the same temperature. In all cases the ultrasonic welding machine HiQ DIALOG 1200 from Herrmann Ultrasonics was employed. The force during vibrations and duration of vibrations were varied to find out the limits between too weak, good, and damaged embossings as shown in Figs. 13, 14, 15, 16, 17 and 18. All other parameters were fixed for all experiments and are shown in Table 1 as process 4.

The comparison of Figs. 13 and 14 shows that the pre-structured foils generating heat in the upper part of the foil stack ease ultrasonic hot embossing. With pre-structured foils, good embossings are obtained at shorter times and at less force. Although the maximum duration of vibrations still yielding good embossings is shorter than with even foils, the process window is much larger with the pre-structured foil.

Fig. 13 Process window of ultrasonic hot embossing of PC foils with the pre-structured surface facing an even foil on top. *Red squares* denote not complete embossing, *brown rhombs* damaged micro structures, and *green circles* good embossing

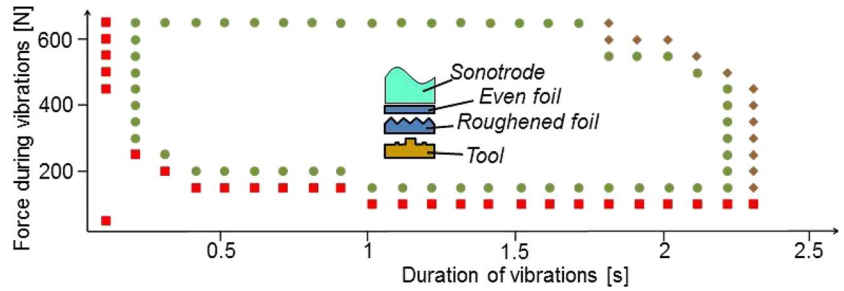


Fig. 14 Process window of ultrasonic hot embossing of PC foils with three even foils

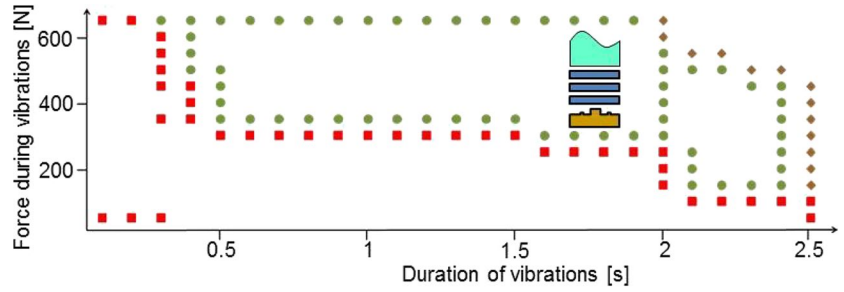


Fig. 15 Process window of ultrasonic hot embossing of PC foils with a pre-structured surface facing the sonotrode

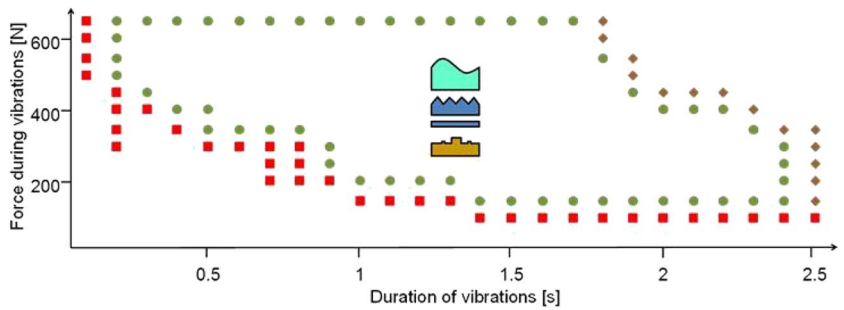


Fig. 16 Process window of ultrasonic hot embossing of PC foils with a pre-structured surface facing the tool

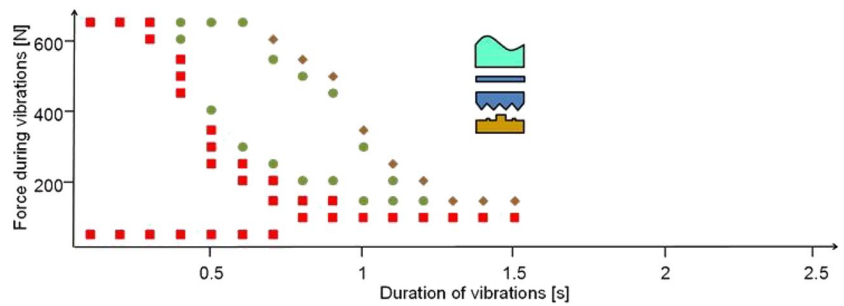
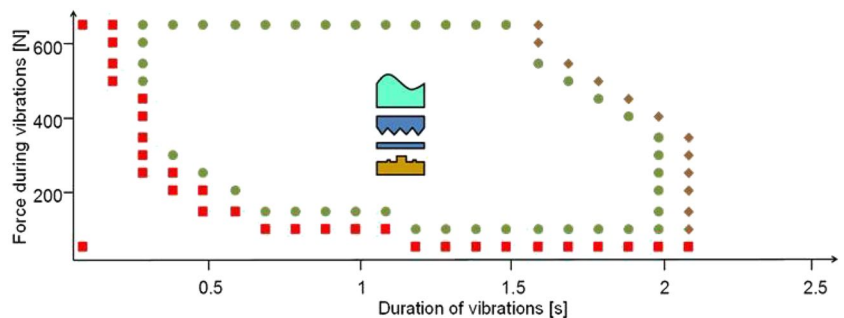


Fig. 17 Process window of ultrasonic hot embossing of PC foils with a pre-structured surface facing an even foil above the tool



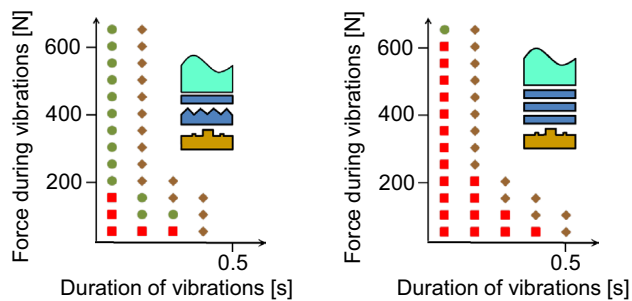


Fig. 18 Process windows of ultrasonic hot embossing of pre-structured and even PVC foils

If the pre-structured foil is facing the sonotrode as shown in Fig. 15, the process window is not enlarged as much as in the case shown in Fig. 13 but still larger than without pre-structures. This is interpreted such that at the interface between sonotrode and polymer friction-heat is generated anyway. Therefore, less extra heating by the pre-structures is required.

When the pre-structures are facing the tool (Fig. 16), the process window is reduced significantly. The required force is a bit reduced when the duration of vibrations are around 1 s, however the micro structures generated by ultrasonic hot embossing are damaged at much shorter times than in any other of the investigated cases and the minimum times of ultrasonic vibrations required are longer even compared to the case without any pre-structured foils (Fig. 14). This may be interpreted such, that additional friction heat is generated at the interface of polymer and tool where it is not required because anyway there is the interface with the largest heat generation. Besides this, the acoustic energy absorbed at the interface is not reflected at the tool anymore and no longer available for heating up the polymer layers above.

The process window shown in Fig. 17, where the pre-structures are facing an even foil above the tool is somehow between the ones shown in Figs. 13 and 15 indicating that additional heat is required most in the upper third of the polymer stack.

The larger the force during the ultrasonic vibrations, the larger is the generated power because the vibration amplitude was kept constant for all experiments and the energy is calculated as the integral of the force times the path. The energy available for heating up and melting the polymer is approximately proportional to the product of the power and the duration of the vibrations. Therefore, a larger force can compensate a shorter vibration time. And the limits of the process windows have to be expected as lines of constant energy in the graphs indicating the energies required for softening and decomposing the polymer. Thus the limits of the process windows are approximately

proportional to the inverse of the duration of vibrations. These curves are shifted in the graphs when the acoustic energy is not absorbed at the optimum locations in the polymer stack decreasing the process window. The optimum locations are expected to be a function of the micro structure design because polymer flow will be required at different locations.

Decomposition of a polymer is not only a function of energy (or temperature) but also of time. This might be the reason why the decomposition limit in Figs. 13, 14, 15 and in Fig. 17 below a certain force is a straight vertical line.

Figure 18 shows the process windows obtained for foils from PVC. For decomposition of PVC much less energy is required, and therefore, a useful process window was opened up only when pre-structures were employed in the upper third of the polymer stack. Both polymers are amorphous (Lechner et al. 2015). But the glass transition temperature of PVC is only half as high as that of PC. Moreover, PVC begins to split off hydrogen chloride at a temperature of 100 °C (Lechner et al. 2015). That might be the reason, why for PVC much less energy is sufficient to destroy it.

All process windows are also a function of the design of the micro structures to be generated. Therefore, the results shown above are not more than an example how the process windows look like. On the other hand, it is expected that the relative changes of process windows of other designs and polymers as a function of pre-structures will be similar and the results shown in this paper will help to find a suitable arrangement of pre-structured foils to improve the process window for other cases.

6 Conclusions

Temperature is a key parameter in all thermoplastic molding processes. This is especially crucial for ultrasonic hot embossing because the polymer is heated up only partially. As a consequence, this process can be influenced comparatively much by steering the absorption of ultrasound by pre-structured foils, foils with different roughness, the order and thickness of polymer layers, powder between polymer layers, and the combination of layers from different polymer materials. This way, the temperature distribution inside of a stack of polymer layers can be adapted to the needs of special tool designs and polymer properties.

This paper also shows that the temperature distribution during ultrasonic processing can be measured with foils from the pyro-electric polymer PVDF and that, this way, the effect of changes in the polymer layers on heat generation can be measured. Temperature measurements with PVDF foils are limited by the Curie temperature of the material and by damages to the sensor foils when the

deformation of the polymer layers starts. PVDF foils could possibly also be employed for temperature measurements in similar processes such as hot embossing (without ultrasound), thermoforming, and injection molding.

It has also been shown that powder can be selectively applied to certain locations in a stack of polymer layers (also in the lateral direction) enhance absorbing ultrasonic energy and generating melt. By pre-structuring certain layers in PC or PVC foil stacks (both polymers are amorphous), process windows can be enlarged or decreased. By pre-structuring of the individual layers in the foil stack, it is finally possible to obtain a more stable manufacturing process for the production of ultrasonic hot embossed microsystems. The limits of the process windows are approximately proportional to the inverse of the vibration time of the sonotrode. If this is assumed, the measuring points on the curves are characterized by constant energy. Thus, a longer vibration time can compensate a lower force, if the polymer is not decomposed quickly like PVC.

Acknowledgments The results presented here were partly achieved with the support of Deutsche Forschungsgemeinschaft with the support code SCHO 850/4 and by a scholarship provided by Erasmus+, and grant (No. MIP-026/2014) from the Research Council of Lithuania, and China Scholarship Council with award no. 2011683003. The test powder was provided by Mr. Gingter, Institute of Mineral Engineering (GHI) at RWTH Aachen University.

References

- Altmann B, Ahrens R, Welle A, Dingreiter H, Schneider M, Schober A (2012) Microstructuring of multiwell plates for three-dimensional cell culture applications by ultrasonic embossing. *Biomed Microdevices* 14:291–301. doi:[10.1007/s1054401196058](https://doi.org/10.1007/s1054401196058)
- Fairbanks HV (1974) Applying ultrasonics to the moulding of plastic powders. *Ultrasonics* 12(1):22–24. doi:[10.1016/0041-624X\(74\)90082-1](https://doi.org/10.1016/0041-624X(74)90082-1)
- Heckele M, Schomburg WK (2004) Review on micro molding of thermoplastic polymers. *J Micromech Microeng* 14:R1–R14. doi:[10.1088/0960-1317/14/3/R01](https://doi.org/10.1088/0960-1317/14/3/R01)
- Hesse S, Schnell G (2014) Sensoren für die Prozess- und Fabrikautomation. 6. Auflage, Springer Vieweg. doi:[10.1007/978-3-658-05867-8](https://doi.org/10.1007/978-3-658-05867-8)
- Khuntontong P, Blaser T, Schomburg WK (2008) Ultrasonic micro hot embossing of thermoplastic polymers. In: Proc. 24th Annual Meeting of the Polymer Processing Society, PPS24, Salerno, Italy, June 15–19, pp II.364
- Lechner MD, Gehrke K, Nordmeier EH (2015) Makromolekulare Chemie. 5. Auflage, Springer-Verlag Berlin Heidelberg. doi:[10.1007/978-3-7643-8891-1](https://doi.org/10.1007/978-3-7643-8891-1)
- Lee CH, Jung PG, Lee SM, Park SH, Shin BS, Kim J-H, Hwang K-Y, Kim KM, Ko JS (2010) Replicaion of polyethylene nano-micro hierachical structures using ultrasonic forming. *J Micromech Microeng* 20(3):035018. doi:[10.1088/0960-1317/20/3/035018](https://doi.org/10.1088/0960-1317/20/3/035018)
- Liao S, Gerhardy C, Sackmann J, Schomburg WK (2015) Tools for ultrasonic hot embossing. *Microsyst Technol* 21(7):1533–1541. doi:[10.1007/s00542-014-2232-6](https://doi.org/10.1007/s00542-014-2232-6)
- Liu S-J, Dung Y-T (2005) Hot embossing precise structure onto plastic plates by ultrasonic vibration. *Polym Eng Sci* 45:915–925. doi:[10.1002/pen.20357](https://doi.org/10.1002/pen.20357)
- Mekaru H, Nakamura O, Maruyama O, Maeda R, Hatt T (2007a) Development of precision transfer technology of atmospheric hot embossing by ultrasonic vibration. *Microsyst Technol* 13(3–4):385–391. doi:[10.1007/s00542-006-0203-2](https://doi.org/10.1007/s00542-006-0203-2)
- Mekaru H, Goto H, Takahashi M (2007b) Development of ultrasonic micro hot embossing technology. *Microelectron Eng* 84:1282–1287. doi:[10.1016/j.mee.2007.01.235](https://doi.org/10.1016/j.mee.2007.01.235)
- Paul DW, Crawford RJ (1981) Ultrasonic moulding of plastic powders. *Ultrasonics* 19(1):23–27. doi:[10.1016/0041-624X\(81\)90028-7](https://doi.org/10.1016/0041-624X(81)90028-7)
- Planellas M, Sacristán M, Rey L, Olmo C, Aymamí J, Casas MT, del Valle LJ, Franco L, Puiggali J (2014) Micro-molding with ultrasonic vibration energy: new method to disperse nanoclays in polymer matrices. *Ultrason Sonochem* 21(4):1557–1569. doi:[10.1016/j.ulsonch.2013.12.027](https://doi.org/10.1016/j.ulsonch.2013.12.027)
- Sackmann J, Burlage K, Gerhardy C, Memering B, Liao S, Schomburg WK (2015) Review on ultrasonic fabrication of polymer micro devices. *Ultrasonics* 56:189–200, ISSN: 0041-624X. doi:[10.1016/j.ultras.2014.08.007](https://doi.org/10.1016/j.ultras.2014.08.007)
- Šakalys R, Janušas G, Palevičius A, Bendikienė R, Palevičius R (2015) Microstructure replication using high frequency vibro-active pad. *Mechanika* 21:(2) 134–140, ISSN: 1392-1207. doi:[10.5755/j01.mech.21.2.8886](https://doi.org/10.5755/j01.mech.21.2.8886)
- Sinha M, Buckley D (2007) Acoustic properties of polymers. In: Mark J, editor. *Physical properties of polymers handbook*. New York: Springer, pp 1021–1031. doi:[10.1007/978-0-387-69002-5_60](https://doi.org/10.1007/978-0-387-69002-5_60)
- Wise R (2010) Initiation of ultrasonic welding in amorphous thermoplastic polymers. *Conf Join Plast DVS-Berichte* 269:29–43
- Yu HW, Lee CH, Jung PG, Shin BS, Kim J-H, Hwang K-Y, Ko JS (2009) Polymer microreplication using ultrasonic vibration energy. *J Micro/Nanolith MEMS MOEMS* 8(2):021113. doi:[10.1117/1.3129824](https://doi.org/10.1117/1.3129824)